

1 **Effect of tank shape on survival and growth of Pacific bluefin tuna *Thunnus***
2 ***orientalis* larvae**

3 Aung Naing Win¹, Wataru Yamazaki², Takamasa Hasegawa¹, Kentaro Higuchi³,
4 Toshinori Takashi³, Koichiro Gen³, Tetsuya Sumida⁴, Atsushi Hagiwara¹, Yoshitaka
5 Sakakura^{1*}

6 ¹ *Graduate School of Fisheries and Environmental Sciences, Nagasaki University,*
7 *Bunkyo 1-14, Nagasaki 852-8521, Japan*

8 ² *Department of Mechanical Engineering, Nagaoka University of Technology, Niigata*
9 *940-2188, Japan*

10 ³ *Research Center for Tuna Aquaculture, Seikai National Fisheries Research Institute,*
11 *Japan Fisheries Research and Education Agency, Taira 9-1551, Nagasaki 851-2213,*
12 *Japan*

13 ⁴ *Shipping Technology Department, National Institute of Technology, Oshima College,*
14 *Yamaguchi 742-2193, Japan*

15

16 Corresponding author:

17 Yoshitaka Sakakura

18 Graduate School of Fisheries and Environmental Sciences, Nagasaki University, 1-14
19 Bunkyo-machi Nagasaki, 852-8521, Japan

20 *E-mail: sakakura@nagasaki-u.ac.jp

21 **Abstract**

22 We examined the effect of rearing tank shape on survival and growth of Pacific bluefin
23 tuna *Thunnus orientalis* larvae. Cylindrical (1.7×10^3 cm² water surface area; 30 cm deep)
24 and rectangular (1.8×10^3 cm² water surface area; 28 cm deep) tanks (n=3 each) were filled
25 with 50 liters of seawater. One air stone with a 100 ml/min aeration rate was set at the
26 bottom center of each tank. Light intensity at the water surface was 2000 lux with a
27 photoperiod of 24L:0D. Larvae were introduced into each tank at a rate of 10 individuals/l
28 at 2 days post-hatching (dph). Rotifers were fed at 10 individuals/ml and their distribution
29 in tanks was measured. Survival of larvae in cylindrical tanks (CT; $52.7 \pm 5.1\%$) at 8 dph
30 was higher than that in rectangular tanks (RT; $0.8 \pm 0.7\%$, $p < 0.01$). Meanwhile, larvae
31 growth was not significantly different between tank shapes either in body length (CT:
32 4.23 ± 0.26 mm; RT: 4.09 ± 0.20 mm) or dry weights (CT: 95.1 ± 17.6 μ g; RT: 67.7 ± 10.9 μ g).
33 The swimbladder inflation rate of larvae also did not differ significantly between tank
34 shapes (CT: $16.5 \pm 14.5\%$; RT: $56.9 \pm 3.47\%$). Rotifer distribution was higher at tank
35 bottom in both shapes ($p < 0.05$). Two-phase bubbly flow simulations in the tanks revealed
36 that the low-flow area was larger in the RT. The low-flow area at tank bottom varied by
37 tank shape, occurring at the edge of the tank wall on the bottom in the CT, and from the
38 center of the tank (air stone) to the tank wall in the RT. These low-flow areas at tank
39 bottom coincided with areas of higher rotifer distribution, which may be a cause of
40 sinking syndrome in fish larvae. Our results indicate that small-scale (50-l) PBT
41 larviculture experiments can be conducted using a CT with the present aeration system,
42 and that an RT requires an improved aerator in place of the single air stone.

43 **Keywords:** Pacific bluefin tuna; rearing tank shapes; sinking syndrome; survival; flow

45 **1. Introduction**

46 Pacific bluefin tuna (PBT) *Thunnus orientalis* is a commercially important fish in Japan,
47 Korea, Taiwan and the United States (Craig et al., 2017). Aquaculture for PBT utilizes
48 wild-caught juveniles as seedlings (Ottolenghi, 2008), and overfishing of PBT juveniles
49 has led to a decline of the PBT population in the wild (Craig et al., 2017). Recently, the
50 full life cycle of PBT was successfully completed under aquaculture conditions for the
51 increasing demands of PBT seedlings (Sawada et al., 2005). However, high mortality
52 occurred during the first 10 days post-hatching (dph), followed by cannibalism during the
53 late larval and juvenile stages, and high mortality occurred by collision with tank or net
54 walls during the juvenile stage (Sawada et al., 2005). The high mortality during the first
55 10 days is an obstacle that must be solved for mass production of *Thunnus* species to gain
56 a stable large-scale supply of seedlings (Woolley et al., 2013; Nakagawa et al., 2011;
57 Sawada et al., 2005).

58 The sinking syndrome is a main cause of high mortality during the early larval
59 stages in PBT larviculture (Masuma et al., 2011). This occurs when larvae sink to the
60 bottom during dark periods because larval swimming activity is low at night, and their
61 body density is higher than that of seawater (Nakagawa et al., 2011; Tanaka et al., 2009;
62 Takashi et al., 2006). Sinking syndrome occurs in many marine fish larvae, including the
63 striped trumpeter *Latris lineata* (Trotter et al., 2005), greater amberjack *Seriola dumerili*
64 (Teruya et al., 2009), yellowtail kingfish *S. lalandi* (Woolley and Qin, 2013), leopard coral
65 grouper *Plectropomus leopardus* (Takebe et al., 2011), kelp grouper *Epinephelus bruneus*
66 (Ching et al., 2014) and tiger grouper *E. fuscoguttatus* (Ching et al., 2016). Sinking
67 syndrome can be reduced by increasing the aeration rate at night (Tanaka et al., 2018;
68 Nakagawa et al., 2011) and/or creating conditions in which the larvae are suspended

69 within the water column of the rearing tank (Kurata et al., 2017; Ching et al., 2016, 2014;
70 Takebe et al., 2011; Tanaka et al., 2009) and by continuous illumination (Kumon et al.,
71 2018; Kurata et al., 2017).

72 In PBT larviculture, water temperature (Tanaka et al., 2018), aeration rates
73 (Tanaka et al., 2018; Kurata et al., 2017; Nakagawa et al., 2011) and light conditions
74 (Kurata et al., 2017) have been studied as physical environmental factors that affect
75 sinking syndrome in PBT larvae. However, information on the effects of tank shape,
76 which affect the early survival of marine fish larvae (Ruttanapornvareesakul et al., 2007)
77 are lacking. In the present study, we hypothesized that tank shape may affect the survival
78 and growth of marine fish larvae. To examine this possibility, we conducted larviculture
79 experiments in small 50-l tanks of different shapes. We chose a cylindrical tank (CT) with
80 axisymmetrical flow field patterns (Sumida et al. 2013), and a rectangular tank (RT) with
81 three-dimensional (3-D) complicated flow field patterns (Takakuwa et al., 2018), to
82 investigate the effect of tank shape on survival and growth of PBT larvae. We also
83 examined the distribution of rotifers to estimate the flow field in tanks, and visualized the
84 flow fields by simulation.

85

86 **2. Materials and Methods**

87 Three blue plastic CT (46 cm in diameter) and blue acrylic RT (60 cm × 30 cm × 35 cm
88 depth) with a 50-l working volume were used in this study. The aspect ratio (liquid
89 depth/internal radius of the tank) of the CT was 1.3. We assumed that the aspect ratio of
90 the RT was also 1.3, since the water surface area and depth of the RT ($1.8 \times 10^3 \text{ cm}^2 \times 28$
91 cm) were almost equal to those of the CT ($1.7 \times 10^3 \text{ cm}^2 \times 30 \text{ cm}$). Tanks were filled with

92 32 parts per thousand (ppt) artificial seawater (Marine Art Hi, Tomita Pharmaceutical,
93 Japan), and placed in a 25 °C temperature-controlled room of the Aquaculture Biology
94 Laboratory, Nagasaki University, Japan. A spherical aerator (5 cm in diameter; 100
95 ml/min aeration rate) was placed at the bottom center of each tank to generate water flow.
96 Light intensity at the water surface was 2000 lux with a photoperiod of 24L:0D to
97 decrease the sinking syndrome that occurs in PBT larvae during dark periods (Nakagawa
98 et al., 2011; Tanaka et al., 2009; Takashi et al., 2006).

99 We followed the PBT larval rearing procedure described by Tanaka et al. (2018), who
100 successfully reared PBT larvae for 7 days dph in 200-l tanks under static conditions (no
101 water exchange). Heavy mortality has been observed within 10 dph in the PBT mass
102 culture process due to the sinking syndrome, and the percentage of sinking PBT larvae
103 on the tank bottom has been shown to peak at around 5 dph (Tanaka et al. 2009). We thus
104 decided on a rearing period of 8 dph. Fertilized eggs of PBT were obtained from Seikai
105 National Fisheries Research Institute, and were transported to the Aquaculture Biology
106 Laboratory, Nagasaki University, Japan, on 30 June 2018. Eggs were first transferred into
107 a 100-l polycarbonate tank and larvae were kept until 2 dph in the same tank at 25 °C and
108 32 ppt. Larvae were distributed into each experimental tank at 10 individuals/l on 2 dph,
109 and reared until 8 dph under static conditions. Super Chlorella V12 (Chlorella Industry
110 Co., Fukuoka, Japan) was added to the experimental tanks as green water, and the density
111 was adjusted to 5×10^5 cells/ml once daily. Rotifers *Brachionus plicatilis* enriched with
112 Super Chlorella V12 were fed to larvae at 10 individuals/ml when the mouth opened (2
113 dph). Water samples to assess rotifer density were collected from 9 stations (3 ml for
114 each) in a vertical cross-section of CTs (Fig. 1(a)) and 27 stations in the quarter segments
115 of RTs (Fig. 1 (b)) using a pipet. Since the rotifer numbers in the experimental tanks

116 increased during the experimental period, we standardized the rotifer distribution in the
117 tanks each sampling day using the following equations:

118
$$\text{deviation value at station } x \text{ on day } i =$$

119
$$\frac{\text{rotifer density at station } x - \text{mean rotifer density on day } i}{\text{standard deviation of rotifer density on day } i} .$$

120 On 8 dph, all surviving larvae in the experimental tanks were counted to calculate
121 the survival rate. Then, about 30 fish in each tank were anaesthetized with 200 ppm of
122 MS222 (Tricaine; Sigma-Aldrich) and observed under a dissecting microscope with
123 transmitted light to see whether the swimbladder was inflated by checking air bubbles in
124 the bladder. Larvae were then fixed with 5% formalin solution. Formalin-preserved fish
125 were individually measured for morphometric characteristics by a digital microscope
126 (VH-6300; Keyence, Osaka, Japan), and then dried at 60 °C for 24 h for measurement of
127 the dry body weight by an ultra-micro balance (UMX2; Mettler Toledo, Columbus, OH,
128 USA).

129 Two-phase bubbly flow simulations were performed in the experimental tanks using
130 a dispersed flow model that was developed by Takakuwa et al. (2018). Its governing
131 equations are composed of the conservation laws of mass and momentum of liquid (water)
132 and gas (air bubble) phases, in which the effects of pressure gradient, drag and lift forces
133 acting on bubbles, gravitational acceleration and flow viscosity are taken into account. A
134 simplified marker and cell (SMAC) method was used to solve the governing equations.
135 For the liquid phase, the free surface was assumed to be flat, and a no-slip boundary
136 condition was used. On the other hand, an outflow condition was given for the gas phase
137 at the free surface. As boundary conditions on the wall surface of tanks, a no-slip
138 condition was given for the liquid phase, while a slip condition was given for the gas
139 phase. An air inlet (square with a side length of 22 mm; aeration rate, 100 ml/min) was

140 set at the center of the bottom surface. The diameter of a bubble was set to 2.0 mm. Flow
141 simulations were performed for 450 s, and averaged flow fields for the last 150 s are
142 discussed in this research.

143 Physical environmental parameters during the experiments were as follows: water
144 temperature 24.3–24.8 °C; salinity 32.1–32.2 ppt; dissolved oxygen 6.2 mg/l; pH 7.94–
145 7.96; and ammonia (NH₃-N) 0.18–0.19 mg/l.

146 2.1 Statistical analysis

147 Differences in the survival, growth and swimbladder inflation rates of larvae between
148 tanks were determined using either Student's *t*-test or Mann-Whitney *U*-test after
149 Shapiro-Wilk normality test. The rotifer distribution in tanks was standardized by the
150 deviation value on day *i*, and determined by two-way ANOVA followed by Tukey HSD
151 test. All analyses used R 3.4.1 software, and a 5% level of confidence was considered a
152 significant difference.

153

154 3. Results

155

156 3.1. Survival, growth and swimbladder inflation of larvae

157 The hatching rate of fish eggs was 100%. The survival rate of PBT larvae at 8 dph in CTs
158 (52.7±5.1%) was significantly higher than in RTs (0.8±0.7%, $p < 0.01$, *t*-test; Table 1).
159 Neither standard length nor dry weight of larvae was significantly different between tank
160 shapes (Table 1). Other morphological parameters of larvae at 8 dph were also not
161 significantly different: total length (CT, 4.23±0.26 mm; RT, 4.09±0.20 mm; $p = 0.9111$, *t*-
162 test, $n = 3$), body depth/standard length (0.18±0.02 mm; 0.17±0.02 mm; $p = 0.8526$, *t*-test,

163 n=3), head length/standard length (0.23 ± 0.01 mm; 0.24 ± 0.02 mm; $p=0.0765$, Mann-
164 Whitney *U*-test, n=3) and eye diameter/standard length (0.11 ± 0.01 mm; 0.11 ± 0.01 mm;
165 $p=0.6667$, Mann-Whitney *U*-test, n=3). The swimbladder inflation rate of larvae was not
166 significantly different between CT and RT (Table 1).

167

168 *3.2 Flow field in the experimental tank*

169 3-D visualizations of streamlines in the rearing tanks are shown in Fig. 2. In the case
170 of the CT, upward flows by the effect of air bubbles generated from the air stone radiated
171 outward in the vicinity of the water surface, and then downward flows were observed
172 along the sidewalls of the tank. A single-pair vortex system could be observed at arbitrary
173 central sections. In the case of the RT, the central upward flows radiated outward in the
174 same manner as the CT. Due to the effect of rectangular corners and the non-axisymmetric
175 shape of the tank, however, a more complicated flow field was generated. Figure 3
176 compares cumulative area distributions of the tanks with respect to the flow velocity
177 magnitude obtained from the flow simulation results. Low-velocity regions in the RT
178 were larger than in the CT regardless of the increasing flow velocity. In Fig. 4, streamlines
179 at the bottom regions (where water depth is more than 25 cm) are visualized, colored by
180 the flow velocity magnitude. In the CT, although low-velocity regions were observed
181 along the outside edge, most streamlines eventually moved toward the center of the tank,
182 which reverted to the upward flow from the air stone. In the RT, the flow velocity
183 magnitude at most bottom regions was larger than the CT, and the flow structures were
184 more complicated. Streamlines from both short sides of the rectangle collided in the
185 vicinity of the center of the long sides, creating a vortex at the upper side of Fig. 4(b), and
186 a large low-velocity area at the lower side of the figure.

187

188 *3.2 Rotifer distribution*

189 Rotifer density increased during the experimental period, reaching 54.7
190 individuals/ml in CT and 52.2 individuals/ml in RT on 8 dph (n=6). Rotifer distribution
191 expressed as an average of deviation values was significantly higher at the edge of the
192 tank wall on the bottom in the CT, and from the air stone to the tank wall on the bottom
193 in the RT ($p<0.05$, Tukey HSD test, n=6; Fig. 5).

194

195 **4. Discussion**

196

197 *4.1 Survival, growth and swimbladder inflation of PBT larvae*

198 The present study examined whether the shape of small-scale larval-rearing tanks affects
199 the survival and growth of PBT larvae, together with the rotifer distribution in tanks. The
200 survival rate of PBT larvae in CTs at 8 dph was about 50-fold higher than that in RTs.
201 Usually, better survival and growth of larvae occurs in large rearing tanks rather than in
202 smaller systems (Houde, 1972). However, the survival rate in this study (52.7%) in the
203 50-l CT under a 24-h photoperiod was higher than that in the 500-l CT of a previous study
204 at 7 dph under natural photoperiod with strong aeration during darkness (about 35%;
205 Tanaka et al., 2018), whose protocol with static conditions was followed here. Survival
206 rates in mass-scale tanks at similar ages were also lower than this study: 19.3% in a 50
207 m³ octagonal tank with a water pump system under a natural photoperiod at 8 dph (Tanaka
208 et al., 2009), and 20.3% in 30 m³ circular tanks with 1.7 l/min aeration rates in daytime
209 and stronger aeration rates (3.0 l/min) during the dark period at 8 dph under a natural

210 photoperiod (Kurata et al., 2014).

211 Moreover, the survival rate in the present study was comparable to that at 10 dph in 1
212 m³ cylindrical fiberglass tanks (22.2–42.3%) with 130 ml/min daytime aeration rates, and
213 1.2 l/min dark-period aeration rates under natural and artificial fluorescent lighting
214 (Kurata et al., 2012), as well as those at 10 dph in 500-l cylindrical polycarbonate tanks
215 (43.2–48.6%) with 300 ml/min daytime aeration rates and 900 ml/min dark-period
216 aeration rates at 12L:12D (Nakagawa et al., 2011). Therefore, we propose that rearing
217 experiments of PBT larvae can be conducted in small-scale tanks in which the rearing
218 environment, such as water temperature and illumination, can be easily manipulated.

219 We did not find significant differences in growth between different rearing tank
220 shapes. Similar findings were reported in the seven-band grouper *Epinephelus*
221 *septemfasciatus* and devil stinger *Inimicus japonicus*, for which the rearing tank shapes
222 affected larval survival but not growth (Ruttanapornvareesakul et al., 2007). The growth
223 of PBT larvae at 8 dph in the present study (about 4.1 mm TL) appeared to be smaller
224 than that of larvae of the same age in previous studies (5.8–6.1 mm: Kurata et al., 2012,
225 2014). Growth measurements were conducted with formalin-fixed specimens in the
226 present study and fresh specimens in Kurata et al. (2012, 2014). If we assume 10%
227 shrinkage in the case of formalin-fixed larvae (Hay, 1982) to the previous studies (Kurata
228 et al., 2012, 2014), body size of our sample (4.1 mm) was still smaller than that of the
229 previous studies (5.2–5.5 mm). The inferior growth of PBT larvae in this study may have
230 been due to the smaller tank volume; thus, we should consider the larval density and water
231 exchange when applying small-scale tanks for PBT larviculture experiments.

232 Sinking syndrome of PBT larvae occurs because larvae with higher body density
233 than seawater sink to the bottom of the tank during dark periods due to low swimming

234 activity (Tanaka et al., 2009; Takashi et al., 2006). Swimbladder inflation failure is one of
235 the causes of sinking syndrome (Kurata et al., 2017, 2015, 2012; Ina et al., 2014; Woolley
236 and Qin, 2013), as the swimbladder controls the buoyancy of fish by reducing body
237 density relative to that of surrounding water (Taylor et al., 2010; Phleger, 1998). However,
238 Takashi et al. (2006) found that the body density of PBT larvae was higher than seawater
239 density during dark periods even in swimbladder-inflated larvae. In the present study, the
240 swimbladder inflation rate varied among tanks but was not significantly different between
241 tank shapes. We presume that swimbladder inflation failure may not be the main cause of
242 sinking syndrome. These results may be in agreement with the present finding that the
243 survival rate in the CT was higher than that in the RT despite the same swimbladder
244 inflation rates between tank shapes. We could not conclusively determine whether
245 swimbladder inflation is directly connected to the cause of sinking syndrome; additional
246 studies with more detailed observations of the diel movement of PBT larvae in the rearing
247 tank will be needed.

248

249 *4.2 Flow field in the cylindrical and rectangular tanks*

250 Unfavorable flow in rearing tanks can cause mass mortality of marine fish larvae
251 (Sakakura et al., 2019; Shiotani et al., 2003; Yamaoka et al., 2000; Backhurst and Harker,
252 1988). Flow field structures in tanks differ by tank size and shape (Sakakura et al., 2019;
253 Moore and Prange, 1994). CTs have an axisymmetrical flow field pattern (Sumida et al.,
254 2013), and the flow field provides a uniform current environment and facilitates the
255 elimination of biosolids from the tank bottom (Masaló and Oca, 2016; Oca and Masaló,
256 2013; Timmons et al., 1998). In the case of RTs, 3-D complicated flow fields and low-
257 flow areas were observed in this study, confirming the findings of a previous study

258 (Takakuwa et al., 2018). Low-velocity areas were larger in the RT, as shown in Fig. 3.
259 Moreover, these low-flow areas and the eddy at the tank bottom coincided with the areas
260 where rotifers were distributed at high density. Thus, the low-flow areas in RTs may be
261 larger at the bottom than in CTs, leading to the sinking syndrome of PBT larvae because
262 low velocities and poor mixing of water in rectangular tanks lead to the creation of
263 stagnate areas, causing the accumulation of biosolids on the tank bottom (Oca and Masalò,
264 2007). These low-flow areas may have negative effects on larviculture (Sakakura et al.,
265 2019).

266 The advantage of numerical modeling of the flow field in a larviculture tank is
267 that we can visualize the field in the rearing tank without a flow meter or intensive labor,
268 and that one established model can be expanded to similarly shaped tanks with different
269 water volumes. Thus, the flow field in similar tank shapes can be easily estimated and the
270 model can help in designing the number and location of aerators and water inlets for the
271 larviculture tank. Our results also demonstrated that comparison of rotifer densities at
272 various sites in a rearing tank could approximately predict the low-flow areas that will
273 cause the sinking syndrome of marine fish larvae.

274

275 In conclusion, the flow field in different larval rearing tank shapes affected the
276 survival of PBT larvae in our experiments. The present study demonstrated that flow field
277 patterns in small-scale CTs (50-l) at $AR=1.3$ are more feasible for the survival of PBT
278 larviculture experiments than those in RTs, and that improvement of aerators beyond a
279 single air stone to decrease low-flow areas at the tank bottom should be developed for
280 RTs.

281

282 **Acknowledgments**

283 The first author is grateful to The Ministry of Education, Culture, Sports, Science and
284 Technology of Japanese Government (Monbukagakusho Scholarships Program) for
285 financial aid. This study was financially supported by a Grant-in-Aid for Scientific
286 Research (19K22338) and by the Strategic Program on Agricultural Research and
287 Innovation of the Ministry of Agriculture, Forestry and Fisheries of Japan.

288

289 **References**

- 290 Backhurst, J.R., and Harker, J.H., 1988. The suspension of feeds in aerated rearing tanks:
291 the effect of tank geometry and aerator design. *Aquac. Eng.* 7: 379-395.
292 [https://doi.org/10.1016/0144-8609\(88\)90002-7](https://doi.org/10.1016/0144-8609(88)90002-7)
- 293 Ching, F.F., Miura, A., Nakagawa, Y., Kato, K., Senoo, S., Sakamoto, W., Takii, K.,
294 Miyashita, S., 2014. Flow field control via aeration adjustment for the enhancement
295 of larval survival of the kelp grouper *Epinephelus bruneus* (Perciformes: Serranidae).
296 *Aquac. Res.* 45: 874-881. <https://doi.org/10.1111/are.12032>
- 297 Ching, F.F., Miura, A., Nakagawa, Y., Kato, K., Sakamoto, W., Takii, K., Miyashita, S.,
298 Senoo, S., 2016. Aeration rate adjustment at night to prevent sinking syndrome-
299 related death in the tiger grouper *Epinephelus fuscoguttatus* (Perciformes:
300 Serranidae) larvae. *Aquac. Res.* 47: 165-175. <https://doi.org/10.1111/are.12479>
- 301 Craig, M., Bograd, S., Dewar, H., Kinney, M., Lee, H.H., Muhling, B., Taylor, B., 2017.
302 Status review report of Pacific bluefin tuna (*Thunnus orientalis*). Report to National
303 Marine Fisheries Service, West Coast Islands Regional Office. 99pp.
- 304 Hay, D. E. 1982. Fixation shrinkage of herring larvae: effects of salinity, formalin

305 concentration, and other factors. *Can. J. Fish. Aquat. Sci.* 39: 1138-1143.
306 <https://doi.org/10.1139/f82-151>

307 Houde, E.D., 1972. Some recent advances and unsolved problems in the culture of marine
308 fish larvae. *Proc. Annu. Work. - World Maric. Soc.* 3: 83–112.
309 <https://doi.org/10.1111/j.1749-7345.1972.tb00050.x>

310 Ina, Y., Sakamoto, W., Miyashita, S., Fukuda, H., Torisawa, S., Takagi, T., 2014.
311 Ontogeny of swim bladder inflation and caudal fin aspect ratio with reference to
312 vertical distribution in Pacific bluefin tuna *Thunnus orientalis* larvae. *Fisheries*
313 *Science* 80:1293-1299. <https://doi.org/10.1007/s12562-014-0809-8>

314 Kumon, K., Tanaka, Y., Ishimaru, C., Sakakura, Y., Eba, T., Higuchi, K., Nishi, A.,
315 Nikaido, H., Shiozawa, S., Hagiwara, A., 2018. Effect of photoperiod on survival,
316 growth and feeding of Pacific Bluefin tuna larvae. *Aquac. Sci.* 66: 177-184 (in
317 Japanese with English abstract). <https://doi.org/10.11233/aquaculturesci.66.177>

318 Kurata, M., Seoka, M., Nakagawa, Y., Ishibashi, Y., Kumai, H., Sawada, Y., 2012.
319 Promotion of initial swimbladder inflation in Pacific bluefin tuna, *Thunnus orientalis*
320 (Temminck and Schlegel), larvae. *Aquac. Res.* 43: 1296-1305.
321 <https://doi.org/10.1111/j.1365-2109.2011.02933.x>

322 Kurata, M., Ishibashi, Y., Takii, K., Kumai, H., Miyashita, S., Sawada, Y., 2014. Influence
323 of initial swimbladder inflation failure on survival of Pacific bluefin tuna, *Thunnus*
324 *orientalis* (Temminck and Schlegel), larvae. *Aquac. Res.* 45: 882-892.
325 <https://doi.org/10.1111/are.12027>

326 Kurata, M., Ishibashi, Y., Seoka, M., Honryo, T., Katayama, S., Fukuda, H., Takii, K.,
327 Kumai, H., Miyashita, S., Sawada, Y., 2015. Influence of swimbladder inflation
328 failure on mortality, growth and lordotic deformity in Pacific Bluefin tuna, *Thunnus*

329 *orientalis*, (Temminck & Schlegel) postflexion larvae and juveniles. *Aquac. Res.* 46:
330 1469-1479. <https://doi.org/10.1111/are.12304>

331 Kurata, M., Tamura, Y., Honryo, T., Ishibashi, Y., Sawada, Y., 2017. Effects of
332 photoperiod and night-time aeration rate on swim bladder inflation and survival in
333 Pacific bluefin tuna, *Thunnus orientalis* (Temminck & Schlegel), larvae. *Aquac. Res.*
334 48: 4486-4502. <https://doi.org/10.1111/are.13274>

335 Masaló, I., Oca, J., 2016. Influence of fish swimming on the flow pattern of circular tanks.
336 *Aquac. Eng.* 74: 84-95. <https://doi.org/10.1016/j.aquaeng.2016.07.001>

337 Masuma, S., Takebe, T., Sakakura, Y., 2011. A review of the broodstock management
338 and larviculture of the Pacific northern bluefin tuna in Japan. *Aquaculture* 315: 2-8.
339 <https://doi.org/10.1016/j.aquaculture.2010.05.030>

340 Moore, A., Prange, M.A., 1994. Evaluation of tank shape and a surface spray for intensive
341 culture of larval walleyes fed formulated feed. *Prog. Fish Cult.* 56: 100-110.
342 [https://doi.org/10.1577/1548-8640\(1994\)056<0100:EOTSAA>2.3.CO;2](https://doi.org/10.1577/1548-8640(1994)056<0100:EOTSAA>2.3.CO;2)

343 Nakagawa, Y., Kurata, M., Sawada, Y., Sakamoto, W., Miyashita, S., 2011. Enhancement
344 of survival rate of Pacific bluefin tuna (*Thunnus orientalis*) larvae by aeration control
345 in rearing tank. *Aquat. Living Resources.* 24: 403-410.
346 <https://doi.org/10.1051/alr/2011150>

347 Oca, J., Masaló, I., 2013. Flow patterns in aquaculture circular tanks: Influence of flow
348 rate, water depth, and water inlet & out features. *Aquac. Eng.* 52: 65-72.
349 <https://doi.org/10.1016/j.aquaeng.2012.09.002>

350 Ottolenghi, F., 2008. Capture-based aquaculture of bluefin tuna. *FAO, Rome.* 508:169-
351 182.

352 Phleger, C., 1998. Buoyancy in marine fishes: direct and indirect role of lipids. *Amer.*

353 Zool. 38: 321-330. <https://doi.org/10.1093/icb/38.2.321>

354 Ruttanapornvareesakul, Y., Sakakura, Y., Hagiwara, A., 2007. Effect of tank proportions
355 on survival of seven-band grouper *Epinephelus septemfasciatus* (Thunberg) and
356 devil stinger *Inimicus japonicus* (Cuvier) larvae. Aquac. Res. 38, 193–200.
357 <https://doi.org/10.1111/j.1365-2109.2007.01653.x>

358 Sakakura, Y., Yamazaki, W., Takakuwa, Y., Sumida, T., Takebe, T., Hagiwara, A., 2019.
359 Flow field control in marine fish larviculture tanks: lessons from groupers and bluefin
360 tuna in Japan. Aquaculture 498: 513-521.
361 <https://doi.org/10.1016/j.aquaculture.2018.09.012>

362 Sawada, Y., Okada, T., Miyashita, S., Murata, O., Kumai, H., 2005. Completion of the
363 Pacific bluefin tuna *Thunnus orientalis* (Temminck et Schlegel) life cycle. Aquac.
364 Res. 36: 413-421. <https://doi.org/10.1111/j.1365-2109.2005.01222.x>

365 Shiotani, S., Akazawa, A., Sakakura, Y., Chuda, H., Arakawa, T., Hagiwara, A., 2003.
366 Measurement of flow field in rearing tank of marine fish larvae: A case study of the
367 seven band grouper *Epinephelus septemfasciatus*. J. Fish. Eng. 39: 205-212 (in
368 Japanese with English abstract). https://doi.org/10.18903/fisheng.39.3_205

369 Sumida, T., Kawahara, H., Shiotani, S., Sakakura, Y., Hagiwara, A., 2013. Observations
370 of flow patterns in a model of a marine fish larvae rearing tank. Aquac. Eng. 57: 24-
371 31. <https://doi.org/10.1016/j.aquaeng.2013.06.002>

372 Takakuwa, Y., Yamazaki, W., Sumida, T., Sakakura, Y., 2018. Flow field investigation in
373 rectangular tanks by bubbly flow simulations. J. Fish. Eng. 54: 155-162 (in Japanese
374 with English abstract). https://doi.org/10.18903/fisheng.54.3_155

375 Takashi, T., Kohno, H., Sakamoto, W., Miyashita, S., Murata, O., Sawada, Y., 2006. Diel
376 and ontogenetic body density change in Pacific bluefin tuna, *Thunnus orientalis*

377 (Temminck and Schlegel), larvae. *Aquac. Res.* 37: 1172-1179.
378 <https://doi.org/10.1111/j.1365-2109.2006.01544.x>

379 Takebe, T., Kobayashi, M., Asami, K., Sato, T., Hirai, N., Okuzawa, K., Sakakura, Y.,
380 2011. Sinking syndrome of larvae of the leopard coral grouper *Plectropomus*
381 *leopardus* and its control for large-scale larviculture. *Fish. Tech.* 3: 107-114 (in
382 Japanese with English abstract).

383 Tanaka, Y., Kumo, K., Nishi, A., Nikaido, H., Eba, T., Shiozawa, S., 2009. Status of the
384 sinking of hatchery-reared larval Pacific bluefin tuna on the bottom of the mass
385 culture tank with different aeration design. *Aquac. Sci.* 57: 587-593.
386 <https://doi.org/10.11233/aquaculturesci.57.587>

387 Tanaka, Y., Kumon, K., Higuchi, K., Eba, T., Nishi, A., Nikaido, H., Shiozawa, S., 2018.
388 Factors influencing early survival and growth of laboratory-reared Pacific bluefin
389 tuna, *Thunnus orientalis*, larvae. *J. World. Aquac. Soc.* 49: 484-452.
390 <https://doi.org/10.1111/jwas.12453>

391 Taylor, G.K., Holbrook, R.I., Perera, T.B.D., 2010. Fractional rate change of swimbladder
392 volume is reliably related to absolute depth during vertical displacements in teleost
393 fish. *J. Royal Soc. Interface.* 7: 1379-1382. <https://doi.org/10.1098/rsif.2009.0522>

394 Teruya, K., Hamasaki, K., Hashimoto, H., Katayama, T., Hirata, Y., Tsuruoka, K.,
395 Hayashi, T., Mushiake, K., 2009. Ontogenetic changes of body density and vertical
396 distribution in rearing tanks in greater amberjack *Seriola dumerili* larvae. *Nippon*
397 *Suisan Gakkaishi* 75: 54-63 (in Japanese with English abstract).
398 <https://doi.org/10.2331/suisan.75.54>

399 Theilacker, G.H., 1980. Rearing container size affects morphology and nutritional
400 condition of larval jack mackerel, *Trachurus symmetricus*. *Fish. Bull.* 78: 789-791

401 Timmons, M.B., Summerfelt, St., Binci, B.J., 1998. Review of circular tank technology
402 and management. *Aquac. Eng.* 18: 51-69. <https://doi.org/10.1016/S0144->
403 [8609\(98\)00023-5](https://doi.org/10.1016/S0144-8609(98)00023-5)

404 Trotter, A.J., Battaglione, S.C., Pankhurst, P.M., 2005. Buoyancy control and diel changes
405 in swim-bladder volume in cultured striped trumpeter (*Latris lineata*) larvae. *Mar.*
406 *Freshwater Res.* 56: 361-370. <https://doi.org/10.1071/MF04209>

407 Woolley, L.D., Qin, J.G., 2013. Ontogeny of body density and the swimbladder in
408 yellowtail kingfish *Seriola lalandi* larvae. *J. Fish Biol.* 82: 658-670.
409 <https://doi.org/10.1111/jfb.12020>

410 Woolley, L.D., Fielder, S.D., Qin, J.G., 2013. Swimbladder inflation associated with body
411 density change and larval survival in southern bluefin tuna *Thunnus maccoyii*.
412 *Aquacult. Int.* 21: 1233–1242. <https://doi.org/10.1007/s10499-013-9626-9>

413 Yamaoka, K., Nanbu, T., Myagawa, M., Isshiki, T., Kusaka, A., 2000. Water surface
414 tension-related deaths in prelarval red-spotted grouper. *Aquaculture* 189: 165-176.
415 [https://doi.org/10.1016/S0044-8486\(00\)00354-9](https://doi.org/10.1016/S0044-8486(00)00354-9)

416

417 **Figure captions**

418 Fig. 1. Sites for rotifer distribution in (a) a cylindrical tank, and (b) a rectangular tank.

419 One air stone was set at the center of the tank bottom.

420

421 Fig. 2. Three-dimensional streamlines predicted in this study in (a) a cylindrical tank (ϕ
422 46 cm \times 29 cm depth), and (b) a rectangular tank (60 \times 30 \times 28 cm depth) with an
423 aerator at the center of the bottom with 100 ml/min aeration.

424

425 Fig. 3. Cumulative area (%) of the velocity magnitude ($< x$ mm/s) between the tanks
426 applied in this study. For instance, the water mass having a velocity between 0–10
427 mm/s occupied 40% and 65% of total water volume in the CT and RT in this study,
428 respectively.

429

430 Fig. 4. Visualization of streamlines at bottom regions of (a) a cylindrical tank (ϕ 46 cm),
431 and (b) a rectangular tank (60 \times 30 cm) in this study. An air stone was located at the
432 center of each graph.

433

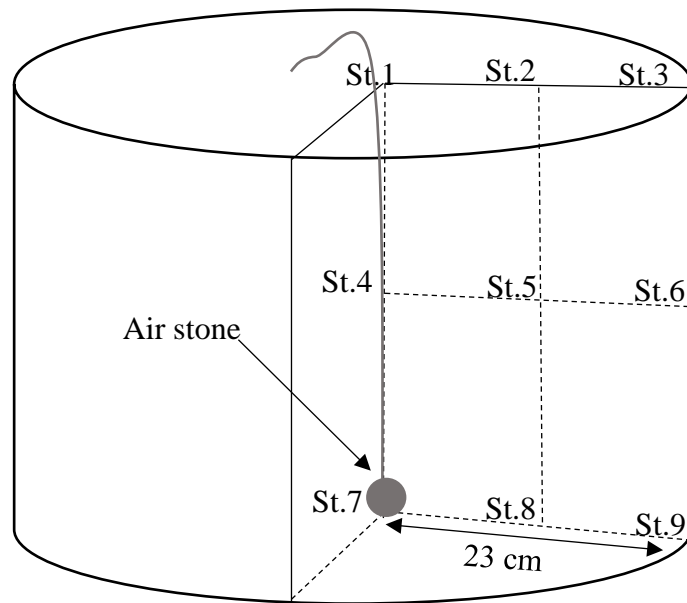
434 Fig. 5. Rotifer distribution (a) at half-cross section in the CT, and (b) in the quadrisection
435 in the RT. Values are average of deviation values during the culture period (n=6,
436 a>b>c>d, Tukey HSD, $p<0.05$).

1 **Table. 1.** Survival, growth and swimbladder inflation rates of *T. orientalis* larvae at 8 dph
2 in tanks of different shapes

Tank	n	Survival (%) *	Standard length (mm)	Dry weight (μg)	Swimbladder inflation (%)
Cylindrical	3	52.7 \pm 5.1	4.06 \pm 0.25	95.1 \pm 17.6	16.5 \pm 14.5 (n=30)
Rectangular	3	0.8 \pm 0.7	3.91 \pm 0.20	67.7 \pm 10.9	56.9 \pm 37.4 (n=1-8)

3 Results are mean values \pm SD. The asterisk indicates a significant difference by *t*-test (*p*
4 < 0.01).

(a)



(b)

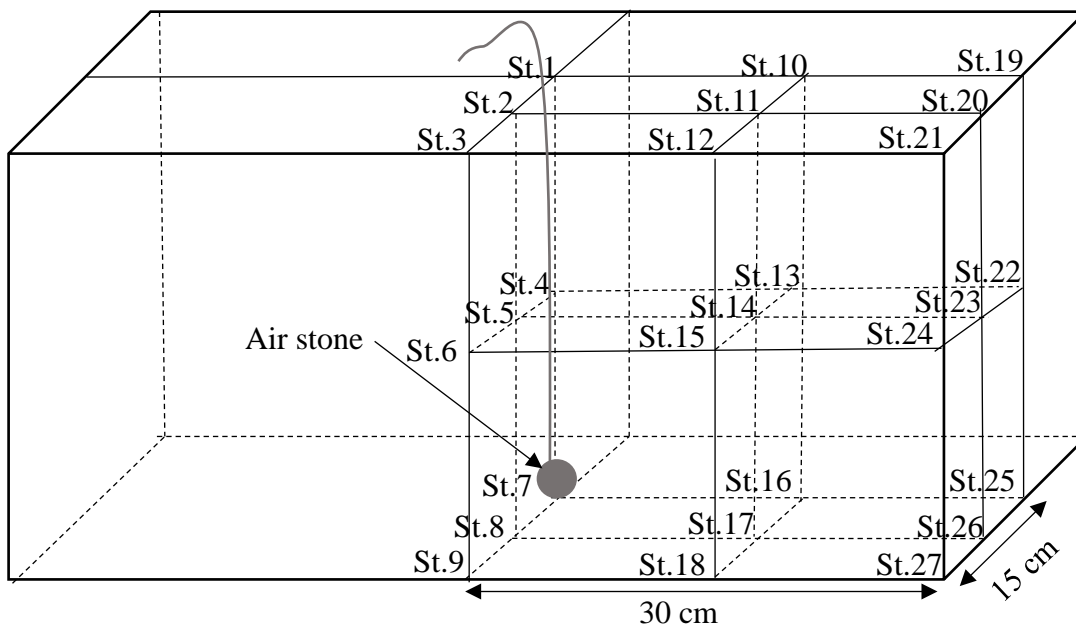
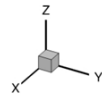
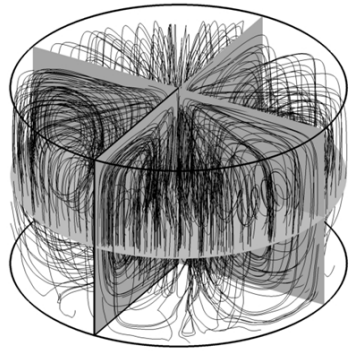


Fig. 1.

(a)



(b)

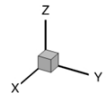
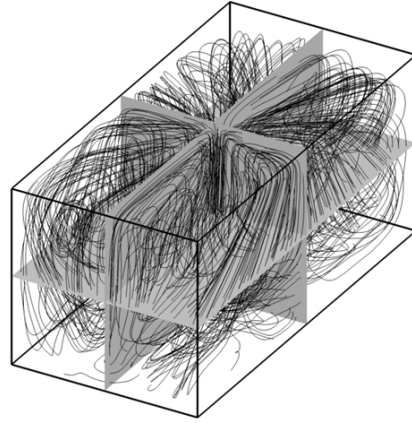


Fig. 2.

Fig. 3.

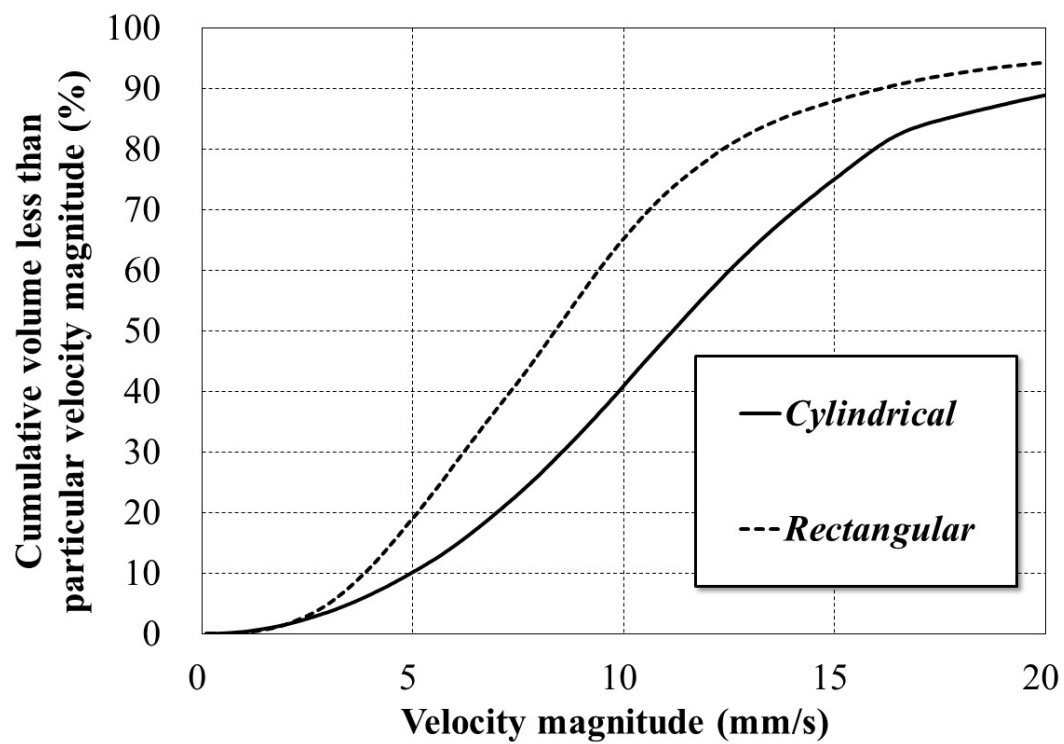


Fig. 4.

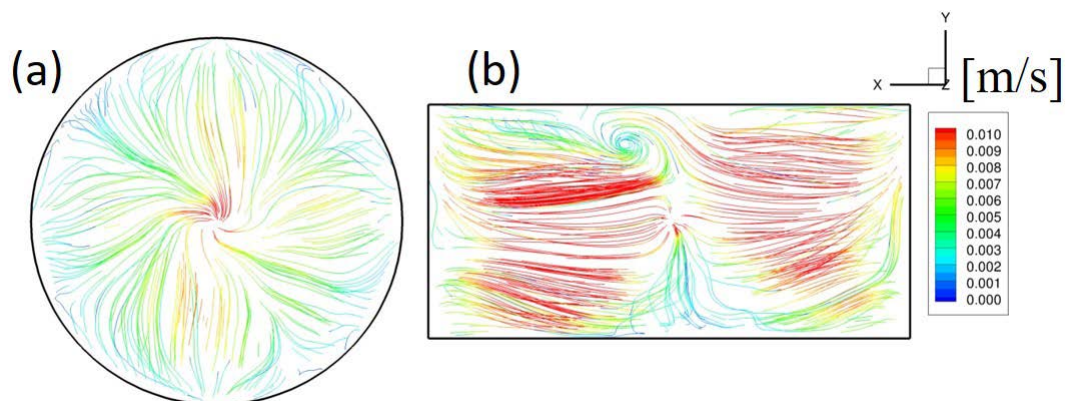
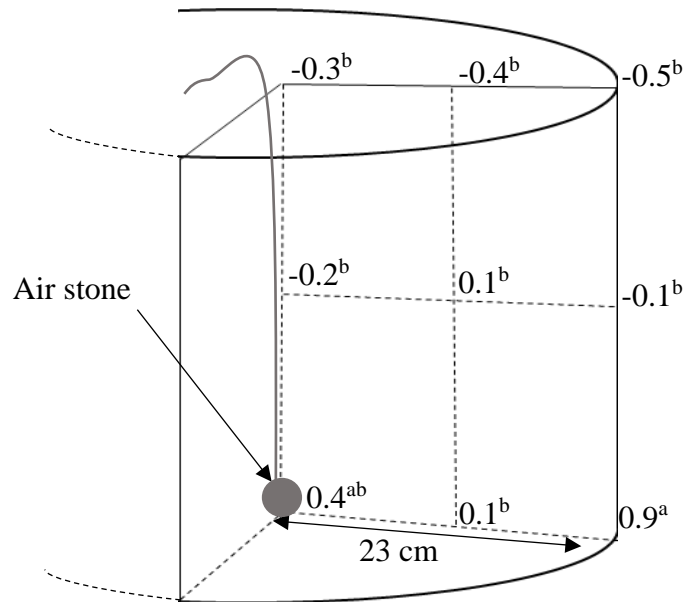


Fig. 5.

(a)



(b)

